

# Zero-Point Corrections and Temperature Dependence of HD Spin–Spin Coupling Constants of Heavy Metal Hydride and Dihydrogen Complexes Calculated by Vibrational Averaging

Brendan C. Mort and Jochen Autschbach\*

Contribution from the Department of Chemistry, University at Buffalo,  
State University of New York, Buffalo, New York 14260-3000

Received December 20, 2005; E-mail: jochena@buffalo.edu

**Abstract:** Vibrational corrections (zero-point and temperature dependent) of the H–D spin–spin coupling constant  $J_{\text{HD}}$  for six transition metal hydride and dihydrogen complexes have been computed from a vibrational average of  $J_{\text{HD}}$  as a function of temperature. Effective (vibrationally averaged) H–D distances have also been determined. The very strong temperature dependence of  $J_{\text{HD}}$  for one of the complexes,  $[\text{Ir}(\text{dmpm})\text{Cp}^*\text{H}_2]^{2+}$  (dmpm = bis(dimethylphosphino)methane) can be modeled simply by the Boltzmann average of the zero-point vibrationally averaged  $J_{\text{HD}}$  of two isomers. For this complex and four others, the vibrational corrections to  $J_{\text{HD}}$  are shown to be highly significant and lead to improved agreement between theory and experiment in most cases. The zero-point vibrational correction is important for all complexes. Depending on the shape of the potential energy and  $J$ -coupling surfaces, for some of the complexes higher vibrationally excited states can also contribute to the vibrational corrections at temperatures above 0 K and lead to a temperature dependence. We identify different classes of complexes where a significant temperature dependence of  $J_{\text{HD}}$  may or may not occur for different reasons. A method is outlined by which the temperature dependence of the HD spin–spin coupling constant can be determined with standard quantum chemistry software. Comparisons are made with experimental data and previously calculated values where applicable. We also discuss an example where a low-order expansion around the minimum of a complicated potential energy surface appears not to be sufficient for reproducing the experimentally observed temperature dependence.

## 1. Introduction

Ever since the isolation and characterization of the first transition metal dihydrogen complex by Kubas and co-workers in 1984,<sup>1</sup> scientists have been fascinated with these types of complexes due to their importance and utility in catalytic reactivity, elusive structure determination, and interesting quantum behavior.<sup>2–10</sup> The understanding of metal dihydride and dihydrogen complexes has long benefited from an “effective interplay” between experiment and theory.<sup>5,11</sup>

Finding methods for conveniently determining the internuclear H–H distance ( $r_{\text{HH}}$ ) in these complexes has been fraught with

some difficulties. First, there is the difficulty of X-ray diffraction of locating the small hydrogen electron density peaks near the metal center. Second, neutron diffraction is not as readily available as X-ray diffraction, and some complexes are not responsive to the technique. Additionally, neutron diffraction can sometimes yield structures that are highly uncertain due to thermal motion. Heinekey and Luther<sup>12</sup> and Maltby et al.<sup>13</sup> have shown the existence of an empirical inverse relationship between the H–H distance and the spin–spin coupling constant  $J_{\text{HD}}$ . The relationship has been improved further by others and is known as the Limbach/Chaudret correlation.<sup>14–16</sup> From a practical point of view, the prediction of  $r_{\text{HH}}$  from NMR solution measurements of  $J_{\text{HD}}$  would allow a convenient characterization of metal dihydrogen, dihydride, and trihydride complexes without resorting to more expensive and difficult techniques. An important factor is to understand the relationship between  $r_{\text{HH}}$  and  $J_{\text{HD}}$  for these complexes.

Computational studies have been carried out to obtain accurate values for the internuclear H–H distance and the spin–spin coupling constant. Density functional theory (DFT) has

- (1) Kubas, G. J.; Ryan, R. R.; Swanson, B. I.; Vergamini, P. J.; Wasserman, H. J. *J. Am. Chem. Soc.* **1984**, *106*, 451–452.
- (2) Maseras, F.; Lledós, A.; Clot, E.; Eisenstein, O. *Chem. Rev.* **2000**, *100*, 601–636.
- (3) Heinekey, D. M.; Oldham, W. J. *J. Chem. Rev.* **1993**, *93*, 913–926.
- (4) Morris, R. H.; Jessop, P. G. *Coord. Chem. Rev.* **1992**, *121*, 155–289.
- (5) Kubas, G. J. *Metal Dihydrogen and  $\sigma$ -Bond Complexes: Structure, Theory, and Reactivity*; Kluwer: New York, 2001.
- (6) Gelabert, R.; Moreno, M.; Lluch, J. M.; Lledós, A. *Organometallics* **1997**, *16*, 3805–3814.
- (7) Eckert, J.; Webster, C. E.; Hall, M. B.; Albinati, A.; Venanzi, L. M. *Inorg. Chim. Acta* **2002**, *330*, 240–249.
- (8) Gelabert, R.; Moreno, M.; Lluch, J. M.; Lledós, A. *J. Am. Chem. Soc.* **1997**, *119*, 9840–9847.
- (9) Gelabert, R.; Moreno, M.; Lluch, J. M.; Lledós, A. *J. Am. Chem. Soc.* **1998**, *120*, 8168–8176.
- (10) Heinekey, D. M.; Lledós, A.; Lluch, J. M. *Chem. Soc. Rev.* **2004**, *33*, 175–452.
- (11) Kubas, G. J. *J. Organomet. Chem.* **2001**, *635*, 37–68.

- (12) Heinekey, D. M.; Luther, T. A. *Inorg. Chem.* **1996**, *35*, 4396–4399.
- (13) Maltby, P. A.; Schlaf, M.; Steinbeck, M.; Lough, A. J.; Morris, R. H.; Klooster, W. T.; Koetzle, T. F.; Srivastava, R. C. *J. Am. Chem. Soc.* **1996**, *118*, 5396–5407.
- (14) Hush, N. S. *J. Am. Chem. Soc.* **1997**, *119*, 1717–1719.
- (15) Gründemann, S.; Limbach, H. H.; Butkowsky, G.; Sabo-Etienne, S.; Chaudret, B. *J. Phys. Chem. A* **1999**, *103*, 4752–4754.

proven to be a useful method for computing electronic and NMR properties of metal complexes such as of interest here.<sup>17</sup> Gusev has recently carried out extensive work on calculating  $J_{\text{HD}}$  for a series of heavy metal hydride and dihydrogen complexes using a hybrid density functional.<sup>18</sup> Le Guennic et al. have subsequently calculated  $J_{\text{HD}}$  for heavy metal dihydrogen and dihydride complexes using gradient-corrected nonhybrid density functionals.<sup>19</sup> Values obtained by both methods appear to average out to similar results. However, the nonhybrid functionals tend to overestimate  $J_{\text{HD}}$  for complexes with small  $r_{\text{HH}}$ . In ref 19 it was concluded that scalar relativistic calculations (i.e. excluding expensive spin–orbit coupling terms) will be sufficiently accurate for correctly reproducing  $J_{\text{HD}}$  within the accuracy limits of standard density functionals.

As a major source of error, these studies did not take into account vibrational corrections in the calculation of the spin–spin coupling constants and were not able to consider any temperature dependence. However, as one might expect for couplings between light nuclei, it has been demonstrated that vibrational corrections to spin–spin coupling constants can be sizable.<sup>20</sup> Regarding dihydrogen and dihydride complexes, in ref 19 it was suggested that the relative magnitude of vibrational corrections to  $J_{\text{HD}}$  might be of particular importance for the interesting crossover region between the dihydrogen and dihydride regimes. The reason for this lies in the weak but still intact H–H bond with a concomitant small coupling constant (as compared to  $\text{H}_2$ ) and rather shallow and likely anharmonic potentials along the H–H stretch coordinate. Such a potential energy surface might also lead to a noticeable temperature dependence of  $J_{\text{HD}}$  due to a temperature-dependent population of vibrational states with differing average spin–spin coupling constants.

As one particularly interesting example, Pons and Heinekey reported the pronounced observable temperature dependence of  $J_{\text{HD}}$  for  $[\text{Ir}(\text{dmpm})\text{Cp}^*\text{H}_2]^{2+}$ , (dmpm = bis(dimethylphosphino)methane), **1**.<sup>21</sup> They attributed this unusual behavior to a rapidly established equilibrium of two isomers, namely an Ir(III) dihydrogen isomer and an Ir(V) *cis*-dihydride isomer. Since decreasing  $J_{\text{HD}}$  values correspond to an increase in  $r_{\text{HH}}$ , they attributed a relatively lower  $J_{\text{HD}}$  value of complex **1** to an equilibrium preference at lower temperatures for the larger H–H distance characteristic of dihydride complexes. At higher temperatures, larger values of  $J_{\text{HD}}$  were observed. This has been attributed to an increasing population of the dihydrogen isomer, which typically has smaller values of  $r_{\text{HH}}$ . Gelabert et al. have subsequently performed a one-dimensional nuclear dynamics calculation on complex **1** to show that a strongly anharmonic double-minimum potential energy surface (PES) results in the temperature dependence of  $r_{\text{HH}}$ . Using the known correlation factors between  $r_{\text{HH}}$  and  $J_{\text{HD}}$ , it was possible to extract a temperature dependence for  $J_{\text{HD}}$ .<sup>16</sup> In a follow-up study, Gelabert et al. further established that there exists a temperature dependence of  $J_{\text{HD}}$  from first-principles by constructing a  $J_{\text{HD}}$

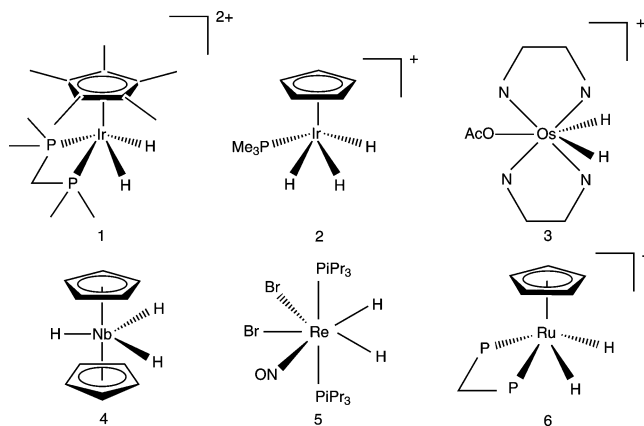


**Figure 1.** The six complexes that were considered in this study.

surface using a two-dimensional nuclear dynamics study.<sup>22</sup> In this latter work, Gelabert et al. confirmed the existence of two minima of complex **1**, corresponding to a *cis*-dihydride and a dihydrogen structure. A two-dimensional cubic spline fit was used to construct a PES and a  $J_{\text{HD}}$  surface from grid points in a plane of H–D and Ir–HD distances. The vibrational average of  $J_{\text{HD}}$  was obtained by integrating the  $J_{\text{HD}}$  surface over the ground state and a few excited-state nuclear wave functions. A Boltzmann average was then applied to these values to establish the temperature dependence of  $J_{\text{HD}}$ . The authors of ref 22 concluded that the PES is very anharmonic, which causes the motion of the H–D and Ir–HD stretches to be temperature dependent. As a result, there is a corresponding temperature dependence of the spin–spin coupling constant which is in qualitative agreement with experiment.

A limitation of applying such an approach straightforwardly to other systems is that two coordinates had to be chosen to represent the nuclear vibrational wave functions. Because the computationally expensive “number crunching” step of the method scales exponentially with the number of coordinates, even considering just one more degree of freedom seems computationally not feasible at present. We have therefore decided to study this complex (**1**), as well as five other complexes shown in Figure 1, with a different approach that we believe leads to a transparent analysis of the  $J$  coupling and its (potential) temperature dependence as long as the potential surface has distinct minima and/or the cubic anharmonicity around the minimum dominates. This computational approach is easy to apply straightforwardly to other systems and other properties. For three of the complexes large differences between DFT calculations and experiment were previously obtained. For another complex, the HD coupling constant is very small (and negative), and it has also turned out to be difficult to obtain calculated results in good agreement with experiment.<sup>18,19</sup> The averaging procedure used here can be seen as complementary to the approach taken by Gelabert et al.<sup>22</sup> because, on one hand, it considers all nuclear degrees of freedom beyond the H–D and M–HD motions but, on the other hand, makes approximations in the way these degrees of freedom are treated.

As a result, we will show that good agreement with experimental  $J_{\text{HD}}$  for five of the complexes in Figure 1 can be obtained by the vibrational averaging of  $J_{\text{HD}}$  over a set of

(16) Gelabert, R.; Moreno, M.; Lluch, J. M.; Lledós, A.; Pons, V.; Heinekey, D. M. *J. Am. Chem. Soc.* **2004**, *126*, 8813–8822.

(17) Bacskey, G. B.; Bytheway, I.; Hush, N. S. *J. Am. Chem. Soc.* **1996**, *118*, 3753–3756.

(18) Gusev, D. G. *J. Am. Chem. Soc.* **2004**, *126*, 14249–14257.

(19) Le Guennic, B.; Patchkovskii, S.; Autschbach, J. *J. Chem. Theory Comput.* **2005**, *1*, 601–611.

(20) Ruden, T. A.; Lutnaes, O. B.; Helgaker, T.; Ruud, K. *J. Chem. Phys.* **2003**, *118*, 9572–9581.

(21) Pons, V.; Heinekey, D. M. *J. Am. Chem. Soc.* **2003**, *125*, 8428–8429.

(22) Gelabert, R.; Moreno, M.; Lluch, J. M.; Lledós, A.; Heinekey, D. M. *J. Am. Chem. Soc.* **2005**, *127*, 5632–5640.

vibrationally excited states, as determined by a Boltzmann distribution. We emphasize that these results were obtained without solving the nuclear Schrödinger equation explicitly (numerically) on a set of grid points in a chosen subspace of the PES. We will analyze some computational strategies for calculating spin–spin coupling constants of these dihydride, dihydrogen, and trihydride complexes with respect to a choice of basis sets. It will also be shown that the temperature dependence of  $J_{\text{HD}}$  for complex **1** can be obtained simply from the Boltzmann average of the temperature-dependent vibrational averaging of the spin–spin coupling constants at the *cis*-dihydride and dihydrogen minima of this system considered as separate species. This leads to a simple interpretation of the temperature dependence mainly as a function of the energy difference between the two minimum structures. Limitations of the approach will be highlighted with the example of complex **6**, where the expansion around the minimum is too near-sighted. Finally, we will construct classifications based on the complexes studied here according to their observed behavior regarding the temperature dependence of the HD spin–spin coupling constant.

## 2. Computational Details

**2.1. Electronic Structure Calculations.** *Gaussian 03*<sup>23</sup> has been used for all density functional theory (DFT) calculations. The  $J_{\text{HD}}$  spin–spin coupling constants were calculated after performing geometry optimizations using very tight convergence criteria. The functionals have been chosen for maximum compatibility with available literature data to facilitate an easy comparison. It should be noted that no dramatic improvement of the results is expected by using other well-established standard hybrid functionals. Frequencies calculations were performed to obtain the normal modes for use in our vibrational averaging program. Technical details of the procedure for obtaining the zero-point vibrational averages have been published elsewhere.<sup>24</sup> The extension to vibrational averaging beyond the zero-point level is outlined in the Supporting Information.

Complex **1** was optimized using the three-parameter hybrid functional of Becke based on the correlation functional of Lee, Yang, and Parr (B3LYP).<sup>25,26</sup> The core shells of the Ir and P atoms have been replaced by the LANL2DZ effective core potential (ECP),<sup>27</sup> and an additional d polarization function was added to the ECP basis for P.<sup>28</sup> The five C atoms of the cyclopentadienyl ring and the bridging C atoms of the dmpm ligand were described by the 6-31G(d) basis set. The 6-31G(p) basis set was used for the H atoms bound directly to the Ir center. The 6-31G basis set was assigned to all other atoms. We have used this method and basis for a direct comparison with the results of ref 22. For a second optimization, the same hybrid functional, pseudopotential, and basis sets were used, except for the H atoms bound to the Ir atom, for which the IGLO-III basis set<sup>29,30</sup> was used. This basis set was designed specifically for NMR chemical shift calculations but has also been successfully applied in hybrid DFT spin–spin coupling constants before.<sup>31</sup> We should note, however, that in ref 22

no large difference was found for  $J_{\text{HD}}$  calculated with the 6-31G(p) and the IGLO-III basis at the same geometry.

Complexes **2**, **3**, **4**, and **5** were optimized using the MPW1PW91 functional which included modified Perdew–Wang exchange and Perdew–Wang 91 correlation.<sup>32–34</sup> The corresponding “Stuttgart/Dresden” SDD basis sets and effective core potentials were used for the Ir, Os, Nb, and Re atoms.

For complex **2**, the 6-31G(d,p) basis set was used for all C, P, and O atoms and for the hydrogen atoms attached directly to the Ir metal. The 6-31G basis set was used for all other H atoms. The 6-31G(d,p) basis set was used for all H, C, N, and O atoms of complex **3**. For complex **4**, the 6-31G(d,p) basis set was used for all C and O atoms and for the H atoms bonded to the Nb metal. The 6-31G basis set was used for the H atoms of the Cp rings. For complex **5**, the 6-31G(d,p) basis set was used for all N, O, and P atoms and for the H atoms attached to the Re metal. The 6-311G(d,f) basis set was used for Br, and 3-21G was used for all other atoms.

Complex **6** was optimized using the three-parameter hybrid functional of Becke based on the correlation functional of Lee, Yang, and Parr (B3LYP).<sup>25,26</sup> The core shells of the Ru atom have been replaced by the LANL2DZ effective core potential (ECP).<sup>27</sup> The 6-31G basis set was used for all atoms, except for the P atoms and the H atoms bound directly to the Ru atom. For the phosphorus atoms, the 6-31G(d) basis set was used, while the 6-31G(p) basis set was used for the H atoms bound to the metal. We have used this method and basis for a direct comparison with the results of ref 8.

For a second set of optimizations for complexes **2**, **3**, **4**, and **6**, the same hybrid functional, pseudopotential, and basis sets were used, except for the H atoms bound to the metal atom. In this second case, the IGLO-III basis set<sup>29,30</sup> was used.

We report  $J$  couplings between H and D nuclei unless explicitly stated otherwise. In some cases, experimental data were available for H–T couplings. To facilitate comparisons, couplings involving pairs of isotopes other than H–D were converted to “H–D units” by using ratios of the magneto-gyric ratios (26.7522128, 4.10662791, and  $28.5349779 \times 10^7 \text{ rad}/(\text{T s})$  for H, D, and T, respectively, from ref 35 as quoted in ref 36).

**2.2. Vibrational Averaging and Temperature Dependence.** Experimentally measured molecular properties represent an average over a range of geometries due to the vibrational motion of molecules. Thus, vibrational averaging has become an important factor in improving the accuracy of first-principles molecular property calculations to predict or confirm experimental data. For this work we have developed a program that calculates vibrationally averaged  $J$  couplings as a function of temperature based on calculations with standard quantum chemical software. The nuclear vibrational wave functions are described by harmonic oscillators with cubic anharmonicity included perturbationally to first order. Further aspects of the method used in this work are outlined in the Supporting Information. The effective vibrationally averaged geometries are also obtained in this procedure (zero-point and temperature-dependent) by using the nuclear positions as the property under consideration. In the following, we report the average H–D distances used in the calculations of  $J_{\text{HD}}$ . For comparison with some of the experimental structural data, using the vibrational average of the H–H distance would be more appropriate. However, this would involve another set of computations of vibrational averages while at the same time (a) not yield effective geometries that differ from the

(23) Frisch, M. J. et al. *Gaussian 03*, Revision C.02; Gaussian, Inc., Wallingford, CT, 2004.

(24) Mort, B. C.; Autschbach, J. *J. Phys. Chem. A* **2005**, *109*, 8617–8623.

(25) Lee, C. T.; Yang, W. T.; Parr, R. G. *Phys. Rev. B* **1988**, *37*, 785–789.

(26) Becke, A. D. *J. Chem. Phys.* **1993**, *98*, 5648–5652.

(27) Hay, P. J.; Wadt, W. R. *J. Chem. Phys.* **1985**, *82*, 299–310.

(28) Hollwarth, A.; Bohme, M.; Dapprich, S.; Ehlers, A. W.; Gobbi, A.; Jonas, V.; Kohler, K. F.; Stegmann, R.; Veldkamp, A.; Frenking, G. *Chem. Phys. Lett.* **1993**, *208*, 237–240.

(29) Kutzelnigg, W.; Fleischer, U.; Schindler, M. The IGLO-Method: Ab Initio Calculation and Interpretation of NMR Chemical Shifts and Magnetic Susceptibilities. In *NMR Basic Principles and Progress*, Vol. 23; Diehl, P.; Fluck, E.; Gunther, H.; Kosfeld, R.; Seelig, J., Eds.; Springer-Verlag: Heidelberg, Germany, 1990.

(30) Extensible Computational Chemistry Environment Basis Set Database. URL <http://www.emsl.pnl.gov/forms/basisform.html>.

(31) Sychrovsky, V.; Gräfenstein, J.; Cremer, D. *J. Chem. Phys.* **2000**, *113*, 3530–3547.

(32) Adamo, C.; Barone, V. *J. Chem. Phys.* **1998**, *108*, 664–675.

(33) Perdew, J. P.; Burke, K.; Wang, Y. *Phys. Rev. B* **1996**, *54*, 16533.

(34) Burke, K.; Perdew, J. P.; Wang, Y. In *Electronic Density Functional Theory: Recent Progress and New Directions*; Dobson, J. F., Vignale, G., Das, M. P., Eds.; Plenum: New York, 1998.

(35) Harris, R. K. In *Encyclopedia of Nuclear Magnetic Resonance*; Grant, D. M., Harris, R. K., Eds.; John Wiley & Sons: Chichester, 1996; Vol. 5.

(36) WebElements, URL <http://www.webelements.com>.

**Table 1.** H–H Equilibrium Distances  $r_e$ , Equilibrium HD Spin–Spin Coupling Constants  $J_e$ , Zero-Point Vibrationally Averaged Values  $\langle r_{\text{HD}} \rangle_0$ ,  $\langle J \rangle_0$ , and Experimental (exp) and Literature (lit) Values for the Two Isomers of Complex **1**<sup>a</sup>

	1a G//G	1a I//G	1a I//I	1b G//G	1b I//I
$r_e$ (Å)	1.652	1.652	1.650	0.939	0.930
$\langle r_{\text{HD}} \rangle_0$ (Å)	1.604	1.604	1.584	1.037	0.983
$r_{e,\text{lit}}$ (Å)	1.63 <sup>b</sup>	1.63 <sup>b</sup>	–	0.93 <sup>b</sup>	–
$J_e$ (Hz)	4.38	4.71	4.36	30.45	30.72
$\langle J \rangle_0$ (Hz)	5.59	6.05	5.88	25.58	28.63
$J_{e,\text{lit}}$ (Hz)	5.0 <sup>b</sup>	5.4 <sup>b</sup>	–	30.6 <sup>b</sup>	–

<sup>a</sup> G means the 6-31G(p), I means the IGLO-III basis set used for the hydrogens bound to the metal. The basis set indicated to the left of the // notation represents the one that was used to calculate the spin–spin coupling constant, and the basis set to the right of the // notation indicates the basis set that was used for the geometry optimization. All calculations presented here were performed with the B3LYP functional. <sup>b</sup> Reference 22.

H–D averages by much more than the experimental error bars for  $r_{\text{HH}}$  and (b) yield the same trends for comparisons between equilibrium and effective geometries.

For each complex **1** to **6** we have examined the contributions to the zero-point vibrational averaging for low-frequency modes corresponding to hindered rotations from methyl and Cp or Cp\* groups. They appear to be small for the complexes investigated here. However, because of the low frequencies their contributions inflate rapidly with increasing temperature and need to be removed from the vibrational averaging to obtain physically meaningful results since at higher temperatures these groups undergo a quasi-free rotation. A refined theoretical identification and treatment of internal hindered rotations would be beneficial for calculations of vibrational corrections, in particular when considering increasing temperature where the contributions from low-frequency modes gain importance.

### 3. Results and Discussion

**3.1. Complex 1.** Complex **1** is known to exhibit two minimum structures. It is also known that the strong temperature dependence of  $J_{\text{HD}}$  is caused by a temperature-dependent equilibrium between these two isomers that have strongly different H–D distances and therefore strongly different  $J_{\text{HD}}$ .<sup>22</sup> As already mentioned in the Introduction, the complex has been treated by a two-dimensional quantum dynamics method in ref 22 where it was suspected that all vibrational degrees of freedom would be necessary to obtain an increase of  $J_{\text{HD}}$  as strong as that observed experimentally (7.3 Hz at 223 K and 9.0 Hz at 303 K<sup>21</sup>). Complex **1**, therefore, represents a very interesting application for our approach.

In agreement with previous work, a lower energy minimum was found to correspond to the *cis*-dihydride isomer of the complex. The structure label **1a** refers to this *cis*-dihydride isomer of complex **1**, and structure **1b** denotes the dihydrogen isomer of complex **1**. Table 1 summarizes the equilibrium and zero-point vibrationally averaged data of complex **1** and compares our results with those of previous work where applicable. As mentioned in Computational Details, we optimized the complexes with very tight convergence criteria. Due to the shallowness of the minima the equilibrium geometries obtained here differ slightly from those of ref 22. The most important difference between the two basis sets is found for the energy difference between the two minima which will turn out to be crucial for obtaining the correct temperature dependence of  $J_{\text{HD}}$ . The dihydrogen minimum is found to be 2.50 and 1.48 kcal/mol higher in energy as calculated by using the

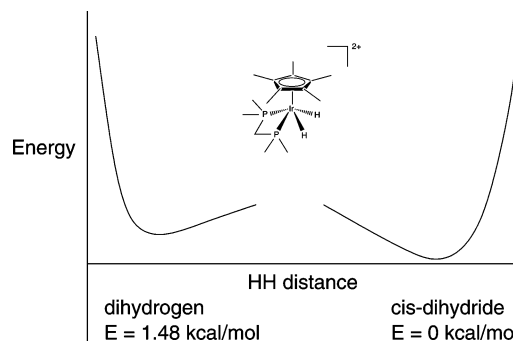


**Figure 2.** A sketch of the potential energy surface for complex **1** along the H–H internuclear distance. The barrier height was not calculated. Shown are the *cis*-dihydride and dihydrogen minima and their energy difference using the 6-31G(p) basis set for the H atoms attached to the Ir metal.

IGLO-III and 6-31G(p) basis sets for the H atoms attached to the metal, respectively. The energy of the barrier between the two isomers was not calculated in this work. It was reported in the literature to be about 0.3 kcal/mol above the dihydrogen minimum.<sup>16</sup>

The zero-point vibrational average of  $J_{\text{HD}}$  for the *cis*-dihydride minimum is 5.88 Hz for the IGLO-III optimized structure and 5.59 Hz for the 6-31G(p) optimized structure, demonstrating that both basis sets yield comparable  $J$  couplings for isomer **1a**. The zero-point vibrational average for the spin–spin coupling constant calculated with the IGLO-III basis set using the 6-31G(p) optimized structure is 6.05 Hz which shows that the difference in  $J_{\text{HD}}$  is not only due to the geometry differences. At the dihydrogen minimum **1b**, the zero-point vibrational average of  $J_{\text{HD}}$  is 25.58 Hz using the 6-31G(p) basis and 28.63 Hz using the IGLO-III basis set. The calculations yield significant zero-point vibrational corrections for  $J_{\text{HD}}$  at both minima.

The vibrational correction for  $J$  consists of two main terms: a correction due to the anharmonicity of the potential ( $\Delta J_a$ ), and a correction due to the curvature of the  $J_{\text{HD}}$  surface as a function of normal coordinates ( $\Delta J_p$ ).<sup>24</sup> The  $\Delta J_a$  term represents the anharmonicity corrections in the nuclear vibrational wave function obtained from “mixing” in other states, as usual in perturbation theory. The signs of the vibrational corrections to the H–D distance for each minimum are compatible with the qualitative shape of the PES around the two minima as shown in Figure 2. The correction for each isomer is in the direction of a less steep increase of the potential. The zero-point vibrational corrections for  $J_{\text{HD}}$  are also in agreement with the empirical relationship between  $r_{\text{HH}}$  and  $J_{\text{HD}}$ , i.e., a positive vibrational correction to  $r_{\text{HH}}$  yields a negative vibrational correction to  $J_{\text{HD}}$ . This behavior appears to indicate that the zero-point corrections to  $J_{\text{HD}}$  for the isomers of complex **1** are dominated by the anharmonicity term  $\Delta J_a$ , but as the detailed data collected in the Supporting Information show, the property curvature term plays an important role as well.

For complex **1** we forego a discussion of the temperature dependence of  $J_{\text{HD}}$  for each minimum separately. The vibrational corrections beyond the zero-point turned out to be small. Depending on the basis set used, the temperature dependencies of  $\Delta J_a$  and  $\Delta J_p$  cancel to some extent for both isomers, but not consistently so. The relative importance of these two terms will be discussed in more detail later for the other complexes. The relevant data for complex **1** are collected in the Supporting

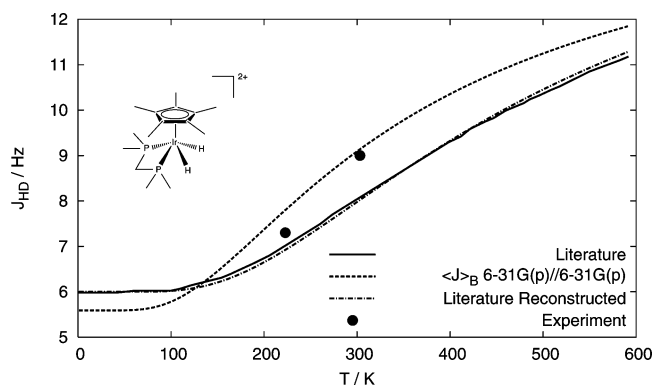


**Figure 3.** Boltzmann average of the zero-point vibrational average of the spin–spin coupling constant at the *cis*-dihydride and dihydrogen minima of complex **1**. The complex was optimized with the 6-31G(p) basis set for the H atoms attached to the Ir metal. See Discussion for details.

Information. It is clear that the vibrational averaging of  $J_{\text{HD}}$  at either minimum cannot reproduce the experimental  $J_{\text{HD}}$  of 7.3 Hz at 223 K and 9.0 Hz at 303 K for the spin–spin coupling constant of complex **1**.<sup>21</sup>

The unusual temperature dependence of  $J_{\text{HD}}$  for complex **1** can be attributed exclusively to a temperature-dependent equilibrium between two isomers of the complex that have a relatively small energy difference and a small barrier for the isomerization. Shown in Figure 3 are the experimental data in comparison with computational results. A Boltzmann average of the zero-point vibrational averages of the spin–spin coupling constants for the two minima calculated for the present work is constructed as a function of temperature using the 6-31G(p) basis. To construct this curve, we have used the equation

$$\langle J \rangle_{\text{B}} = \frac{\langle J \rangle_{0,\text{c}} + \langle J \rangle_{0,\text{d}} e^{-\Delta E/kT}}{1 + e^{-\Delta E/kT}} \quad (1)$$

where  $\langle J \rangle_{0,\text{c}}$  is the zero-point vibrational average of the HD spin–spin coupling constant at the *cis*-dihydride minimum,  $\langle J \rangle_{0,\text{d}}$  is the zero-point vibrational average of  $J_{\text{HD}}$  at the dihydrogen minimum, and  $\Delta E$  is the energy difference between the two minima. We have included in  $\Delta E$  the zero-point vibrational energy (ZPVE) of the two minima for calculating the results shown in Figure 3. The difference between the ZPVE of the two structures is calculated as  $-0.56$  kcal/mol using the 6-31G(p) basis set and therefore of high importance ( $\Delta E + \text{ZPVE} = 0.92$  and  $1.79$  kcal/mol for 6-31G(p) and IGLO-III, respectively).

Included in the plot given in Figure 3 is the graph of the temperature dependence of  $J_{\text{HD}}$ , indicated by “Literature” as calculated recently by Gelabert et al.<sup>22</sup> In the method of Gelabert et al., the nuclear Schrödinger equation was solved in a discrete variable representation. As already mentioned, two coordinates had to be selected for this procedure. They were chosen as the H–D and Ir–HD distances. Ground-state and excited-state vibrational modes for the Ir–HD moiety were then used to construct a temperature dependence of  $J_{\text{HD}}$  through a Boltzmann average over each of the excited nuclear vibrational states based on this PES subspace. However, as mentioned by Gelabert et al., the plot obtained did not consider other (low-lying) vibrational levels that can contribute to the overall temperature dependence of  $J_{\text{HD}}$  for the complex.

Differences between the curve constructed by us using eq 1 and the one reported in the literature can be mainly attributed

to the different equilibrium values that were obtained for the spin–spin coupling constants at the two minima, and to the different value for  $\Delta E$ . Our calculated equilibrium  $J_{\text{HD}}$  of the *cis*-dihydride isomer is 4.38 Hz, while Gelabert et al. report a value of 5.0 Hz. We note that our zero-point vibrational correction is 1.21 Hz, while their correction is 1.0 Hz. The correction obtained here is larger most likely due to the contributions of other normal modes not considered in the nuclear dynamics study of ref 22. The temperature dependence of  $J_{\text{HD}}$  constructed from eq 1 is stronger than the literature curve due to the inclusion of the zero-point vibrational energy from all normal modes in the total energy of the two minima. The differences in the equilibrium coupling constants can be attributed to different convergence criteria and grid selections in the DFT calculations which, as already mentioned, lead to small differences in the equilibrium H–D distances. The importance of obtaining very accurate geometries necessary for the vibrational averaging calculations is reflected by the shallowness of the two minima. Additionally, the Cp\* ring has a rotational energy barrier that is very low, and noticeable geometry changes can result in slight energy changes.

In Figure 3, it is also demonstrated that the temperature dependence of  $J_{\text{HD}}$  as constructed by Gelabert et al. yields essentially the same result as the Boltzmann average of  $J_{\text{HD}}$  for the two minima considered as separate species. We show this by comparing the curve of ref 22 with our curve labeled “Literature Reconstructed”. To construct this curve, we have used a zero-point vibrationally averaged value of 6.0 Hz for the spin–spin coupling constant of the *cis*-dihydride minimum **1a** and 30.6 Hz for the equilibrium value of  $J_{\text{HD}}$  for the dihydrogen minimum **1b**, as reported in ref 22. The energy difference used here is 1.4 kcal/mol as reported in the reference. Since no individual zero-point vibrational average for the spin–spin coupling constant of the dihydrogen minimum was available from ref 22, we have estimated a zero-point contribution  $\Delta J$  (6-31G(p) basis set) that is compatible with the approach used in ref 22. Because Gelabert et al. considered only two degrees of freedom (namely, the Ir–HD and H–D distances) in their study, we have identified two corresponding normal modes of the dihydrogen isomer. We have added a zero-point vibrational correction of  $-1.92$  Hz obtained from our calculations for these modes to the  $J_{\text{HD}}$  equilibrium value of 30.6 Hz from ref 22 to obtain a zero-point vibrationally averaged  $J_{\text{HD}}$  for the dihydrogen isomer **1b** that corresponds as closely as possible to the procedure used in ref 22. We then make use of eq 1 to obtain the “Literature Reconstructed” curve shown in Figure 3. It is seen that the temperature dependence of  $J_{\text{HD}}$  constructed in this manner follows the curve calculated by Gelabert et al. very closely.

The point to be emphasized here is that the construction of the temperature dependence of  $J_{\text{HD}}$  as in ref 22 can be accomplished by a simple Boltzmann average of the zero-point vibrational averages of the two isomers of complex **1**. An explicit quantum nuclear dynamics study appears not to be necessary for obtaining these results as long as two distinct minima can be located. Each zero-point vibrational average calculation then requires twice the number of normal modes gradient and property calculations, which is easily parallelized. The temperature dependence of the average  $J_{\text{HD}}$  for each minimum can be obtained at negligible additional cost, but we

have seen that for complex **1** the separate contributions are too small to be of significance compared to the changes in  $J_{\text{HD}}$  due to the population of the minimum **1b**.

At first sight it is surprising that the temperature-dependent Boltzmann average of the two zero-point averaged coupling constants yields such good agreement with the treatment of ref 22 (provided that equivalent parameters are used). The low barrier between the two minima and the strong anharmonicity of the PES suggest that the first-order perturbative anharmonicity correction in our calculation might not be sufficient. However, the anharmonicity shows up in our treatment in form of large zero-point corrections to  $J_{\text{HD}}$  at each minimum and appears to be described sufficiently accurately (for instance by comparison of the zero-point corrections for isomer **1a** with those of ref 22). A strong delocalization of the quantum nuclear vibrational wave functions over both minima **1a** and **1b** in ref 22 along with a sufficiently small energy separation between the ground state to allow thermal population was mainly obtained for the first excited state (within the 2D subspace of the PES). As a consequence of the delocalization over both minima, this state had a very large vibrational correction to  $J_{\text{HD}}$  which then caused the strong temperature dependence. In our approach, the same situation simply manifests itself in the thermal Boltzmann population of the dihydrogen minimum—with essentially the same numerical results as long as the same energy difference for the two minima and comparable vibrationally averaged  $J_{\text{HD}}$  are used.

The model complex **6** discussed later represents a system where the first-order anharmonicity correction is not sufficient anymore to describe the temperature dependence of  $J_{\text{HD}}$  because there is no distinct second PES minimum for which we can simply assume a thermal Boltzmann population. One would also expect difficulties for a system where two minima are nearly or exactly degenerate and separated by an even smaller barrier.

In ref 22 the authors suggested that other low-lying vibrational states not covered by the 2D approach might lead to a stronger temperature dependence and better agreement with experiment. Our results demonstrate that this is correct. They also reveal in which way these low-lying states affect the temperature dependence of  $J_{\text{HD}}$ : *First*, we find that low-frequency normal modes contribute to the zero-point averages of  $J_{\text{HD}}$  at each minimum, which, along with the equilibrium geometries, define the two “ends”, i.e., the low- $T$  and the high- $T$  limit, of the  $J_{\text{HD}}$  vs  $T$  curve. *Second*, our results show that the shape and the steepness of the  $J_{\text{HD}}$  vs  $T$  curve is mainly determined by the energy difference between the two minima according to eq 1. Here it makes an important difference whether the equilibrium energies for determining  $\Delta E$  are used or if the zero-point vibration energies (ZPVEs) are added. All normal modes contribute to this ZPV energy difference. Our result for complex **1** as shown in Figure 3 (which agrees very well with the experimental data) includes the ZPVEs for the calculation of  $\Delta E$  in the Boltzmann average. Obviously, this energy difference has to be calculated quite accurately to obtain just the right temperature dependence in particular between 200 and 300 K where  $J_{\text{HD}}$  increases most strongly with  $T$ . Further improvement of the results obtained either with our or a quantum dynamics technique may be obtained by considering solvent effects and finite temperature corrections on  $\Delta E$  which, however, is beyond the scope of this work. *Third*, our results show that excited

**Table 2.** H–H Equilibrium Distances  $r_e$ , Equilibrium HD Spin–Spin Coupling Constants  $J_e$ , Zero-Point Vibrationally Averaged Values  $\langle r_{\text{HD}} \rangle_0$ ,  $\langle J \rangle_0$ , and Experimental (exp) and Literature (lit) Values for Complex **2**<sup>a</sup>

	<b>2</b> G/G	<b>2</b> I/I	<b>2</b> I/G
$r_e$ (Å)	1.706	1.699	1.706
$\langle r_{\text{HD}} \rangle_0$ (Å)	1.687	1.675	—
$r_{\text{exp}}$ (Å)	1.69(1) <sup>b</sup>	1.69(1) <sup>b</sup>	1.69(1) <sup>b</sup>
$r_{\text{e,lit}}$ (Å)	1.705 <sup>c</sup>	—	—
$J_e$ (Hz)	2.37	2.76	2.75
$\langle J \rangle_0$ (Hz)	3.05	3.53	—
$J_{\text{exp}}$ (Hz)	3.9 <sup>d</sup>	3.9 <sup>d</sup>	3.9 <sup>d</sup>
$J_{\text{e,lit}}$ (Hz)	2.4 <sup>c</sup>	—	—

<sup>a</sup> For an explanation of the notation, see caption of Table 1. The MPW1PW91 functional was used for all calculations presented here. <sup>b</sup> Reference 37. <sup>c</sup> Reference 18. <sup>d</sup> Reference 38.  $J_{\text{HD}}$  has been converted from a measurement of  $J_{\text{HT}}$ . See text for details.

**Table 3.** Temperature Dependence of the Results for Complex **2** Using the 6-31G(p) Basis Set for Optimization and for Calculation of  $J_{\text{HD}}$ <sup>a</sup>

	0 K	20 K	100 K	200 K	300 K	400 K	600 K
$\Delta r_{\text{HD}}$ (Å)	−0.019	−0.020	−0.032	−0.050	−0.070	−0.092	−0.137
$\langle r_{\text{HD}} \rangle$ (Å)	1.687	1.686	1.674	1.656	1.636	1.614	1.569
$\Delta J_a$ (Hz)	0.310	0.315	0.370	0.449	0.539	0.636	0.845
$\Delta J_p$ (Hz)	0.370	0.381	0.490	0.641	0.809	0.991	1.381
$\Delta J$ (Hz)	0.680	0.696	0.860	1.091	1.348	1.627	2.226
$\langle J \rangle$ (Hz)	3.05	3.07	3.23	3.46	3.72	4.00	4.60
$\langle J \rangle^*$ (Hz)	3.04	3.04	3.11	3.21	3.34	3.49	3.83

<sup>a</sup>  $\Delta r_{\text{HD}}$  is the vibrational correction to the equilibrium H–D distance.  $\langle r_{\text{HD}} \rangle$  is the vibrational average of the H–D distance at the specified temperature. The vibrational correction to the HD spin–spin coupling constant is indicated by  $\Delta J$ . The correction consists of two components: an anharmonic correction ( $\Delta J_a$ ) and a property curvature correction ( $\Delta J_p$ ). The vibrational average of the HD spin–spin coupling constant is denoted by  $\langle J \rangle$ . See the Discussion for more detail. The MPW1PW91 functional was used for all calculations presented here.  $J_e$  is 2.37 Hz. The data marked with an asterisk have the contribution from normal mode 1 (22 cm<sup>−1</sup>) removed (Cp rotations).

vibrational states of the individual isomers provide relatively minor contributions to  $J_{\text{HD}}$  in complex **1** compared to those from the overall strong temperature dependence.

**3.2. Complex 2.** Complex **2** is a trihydride complex that has an experimental H–H distance of 1.69(1) Å.<sup>37</sup> The data for the equilibrium, experimental, literature, and zero-point vibrationally averaged H–D distance and  $J_{\text{HD}}$  spin–spin coupling constants are collected in Table 2. The zero-point vibrationally averaged values for  $\langle r_{\text{HD}} \rangle$  agree comparably well with the experimental H–H distance both for the 6-31G(p) and the IGLO-III basis, assuming an experimental uncertainty of 0.01 Å.

Tables 3 and 4 show the results for the temperature dependence of the vibrational average of  $J_{\text{HD}}$  for complex **2** using the 6-31G(p) and IGLO-III basis sets, respectively. The calculated  $J_{\text{HD}}$  using the IGLO-III basis set at the 6-31G(p) geometry is close to  $J_{\text{HD}}$  obtained with the 6-31G(p) basis set at the 6-31G(p) optimized geometry. This is expected since the spin–spin coupling constant is highly dependent on the geometry used for the calculation. From Table 2, it can be seen that applying the zero-point vibrational correction to the equilibrium  $J_{\text{HD}}$  gives a calculated spin–spin coupling constant that is closer to experiment.<sup>38</sup> It needs to be pointed out that

(37) Heinekey, D. M.; Millar, J. M.; Koetzle, T. F.; Payne, N. G.; Zilm, K. W. *J. Am. Chem. Soc.* **1990**, *112*, 909–919.

(38) Heinekey, D. M.; Hinkle, A. S.; Close, J. D. *J. Am. Chem. Soc.* **1996**, *118*, 5353–5361.

**Table 4.** Temperature Dependence of the Results for Complex **2** Using the IGLO-III Basis Set for Optimization and for Calculation of  $J_{\text{HD}}^a$

	0 K	20 K	100 K	200 K	300 K	400 K	600 K
$\Delta r_{\text{HD}}$ (Å)	-0.024	-0.025	-0.043	-0.068	-0.095	-0.125	-0.185
$\langle r_{\text{HD}} \rangle$ (Å)	1.675	1.674	1.656	1.631	1.604	1.574	1.514
$\Delta J_a$ (Hz)	0.365	0.376	0.479	0.623	0.780	0.948	1.302
$\Delta J_b$ (Hz)	0.402	0.418	0.552	0.735	0.937	1.154	1.617
$\Delta J$ (Hz)	0.767	0.794	1.032	1.358	1.717	2.102	2.919
$\langle J \rangle$ (Hz)	3.53	3.56	3.79	4.12	4.48	4.87	5.68
$\langle J \rangle^*$ (Hz)	3.51	3.52	3.63	3.80	3.99	4.21	4.69

<sup>a</sup> For further details on the notation used, see Table 3, footnote a. The MPW1PW91 functional was used for all calculations presented here.  $J_e$  is 2.76 Hz. The data marked with an asterisk have the contribution from normal mode 1 (19 cm<sup>-1</sup>) removed (Cp rotations).

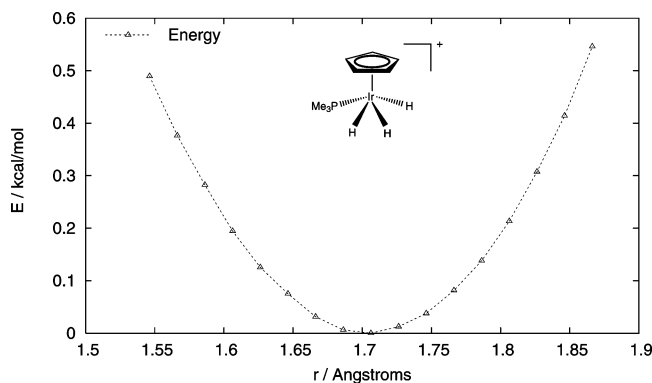


**Figure 4.** Energy of complex **2** as a function of H–H internuclear distance using the 6-31G(p) basis set for the H atoms bound to Ir. Each point of the relaxed PES scan has been optimized with the MPW1PW91 hybrid functional.

the “experimental”  $J_{\text{HD}}$  stems from a measurement of the H–T coupling which we converted to H–D coupling units solely for the purpose of convenience when comparing the coupling constants. For comparison, we have also calculated the vibrationally averaged H–T coupling for the tritium-substituted complex, which affords similar coupling constants but slightly smaller vibrational corrections (see Supporting Information).

For complex **2**, the zero-point vibrationally averaged spin–spin coupling constant calculated using the IGLO-III basis set is closer to the experimental  $J_{\text{HD}}$ . The difference between the equilibrium  $r_{\text{HH}}$  using the 6-31G(p) basis set and the IGLO-III basis set is within 0.01 Å. Likewise, the differences between these two basis sets for the calculation of  $\langle r_{\text{HD}} \rangle_0$  is about 0.01 Å. As a result, there is little difference in the geometry of the H–H distance with respect to the basis sets used for complex **2**. However, the equilibrium and zero-point vibrationally averaged  $J_{\text{HD}}$  spin–spin coupling constants are quite different when comparing the results across the two basis sets. The zero-point vibrational corrections amount to almost 25% of the equilibrium value when considering both basis sets and are therefore highly significant for this complex.

When comparing the vibrationally averaged H–D distance  $\langle r_{\text{HD}} \rangle_0$  to the equilibrium distance  $r_e$  for complex **2**, it is easy to see that the effective distance between the two hydrogen atoms decreases with temperature. This observation indicates that the potential energy surface is steeper in the direction of increasing H–H distance. We have confirmed this by examining the potential energy as a function of  $r_{\text{HH}}$ . A plot for  $E$  vs  $r_{\text{HH}}$  is given in Figure 4. As expected, a positive vibrational correction to  $J_{\text{HD}}$  is also observed. Both basis sets predict the same trend

for the spin–spin coupling constant, i.e., an increase of temperature results in an increase in the spin–spin coupling constant. The experimental H–T coupling converted to  $J_{\text{HD}}$  is 3.9 Hz at  $T = 200$  K. The calculated temperature corrections to  $J_{\text{HD}}$  for this complex turn out to be noticeable over a large temperature range. At 100 K, they represent almost an additional 5% of the zero-point vibrationally averaged  $J_{\text{HD}}$ , and at 400 K, approximately an additional 15–20% of  $\langle J \rangle_0$ . Some of this temperature dependence, however, is due to a low-frequency hindered rotation which should be removed at higher temperatures (see data marked by an asterisk in Table 3). Perhaps a temperature dependence of  $J_{\text{HD}}$  in this complex might be observable experimentally. The H–T coupling has in 1996 been reported by Heinekey et al.<sup>12</sup> as temperature independent between 125 and 200 K. Between 100 and 200 K the predicted change in  $J_{\text{HT}}$  is roughly of the same magnitude as the experimental uncertainties in the  $J_{\text{HT}}$  measurements.<sup>39</sup> Higher-order anharmonicity corrections might also gain importance as  $T$  increases. We plan to investigate soon whether these corrections would be able to partially counterbalance or add to the cubic anharmonic terms considered here.

To assess the accuracy achieved with the two basis sets, we point out that the calculated  $J_{\text{HD}}$  range is small compared to that of complex **1** (Figure 3) and that absolute deviations between theory and experiment on the order of 10% might be expected because of the approximations in the density functional and the basis set which cause errors in the equilibrium coupling constants.<sup>40</sup> Sign and magnitude of the vibrational corrections and the temperature dependence are expected to be reproduced with reasonable accuracy relative to the equilibrium value. Once the zero-point and finite temperature corrections are considered, both basis sets yield acceptable agreement with experiment within the error margins that would be expected for a hybrid density functional applied within an NMR calculation on a transition metal complex.

**3.3. Complex 3.** Complex **3** is an elongated osmium dihydrogen complex with an experimental H–H length of 1.34–(2) Å.<sup>41</sup> The data for the experimental, literature, and calculated  $J_{\text{HD}}$  and  $r_{\text{HH}}$  are shown in Table 5. Also given in the same table is the data for the zero-point vibrational correction to the H–D distance and the spin–spin coupling constant. The zero-point vibrational average of the H–D distance for complex **3** is shorter than the equilibrium distance. Although  $\langle r_{\text{HD}} \rangle_0$  differs noticeably from the experimental H–H distance, the vibrationally averaged HD spin–spin coupling constants are still in good agreement with the experimental  $J_{\text{HD}}$ . Whereas the equilibrium  $J_{\text{HD}}$  is too low, the averaged  $\langle J_{\text{HD}} \rangle$  is too high. The experimental distance was obtained by neutron diffraction, and it has been stated that this technique can sometimes overestimate the H–H distance.<sup>18</sup> If in turn the calculations have a tendency to underestimate this distance in this particular system, we can rationalize not only why the difference between theory and experiment for the geometry is larger here than for the other complexes but also

(39) Heinekey, D. M. Private communication.

(40) Autschbach, J. The calculation of NMR parameters in transition metal complexes. In *Principles and Applications of Density Functional Theory in Inorganic Chemistry I*; Kaltsoyannis, N., McGrady, J. E., Eds.; Springer: Heidelberg, 2004; Vol. 112.

(41) Hasegawa, T.; Li, Z.; Parkin, S.; Hope, H.; McMullan, R. K.; Koetzle, T. F.; Taube, H. *J. Am. Chem. Soc.* **1994**, *116*, 4352–4356.

**Table 5.** H–H Equilibrium Distances  $r_e$ , Equilibrium HD Spin–Spin Coupling Constants  $J_e$ , Zero-Point Vibrationally Averaged Values  $\langle r_{\text{HD}} \rangle_0$ ,  $\langle J \rangle_0$ , and Experimental (exp) and Literature (lit) Values for Complex **3**<sup>a</sup>

	3 G//G	3 I//I	3 I//G
$r_e$ (Å)	1.281	1.263	1.281
$\langle r_{\text{HD}} \rangle_0$ (Å)	1.174	1.156	—
$r_{\text{exp}}$ (Å)	1.34(2) <sup>b</sup>	1.34(2) <sup>b</sup>	1.34(2) <sup>b</sup>
$r_{e,\text{lit}}$ (Å)	1.28 <sup>c</sup>	—	—
$J_e$ (Hz)	6.69	8.29	7.68
$\langle J \rangle_0$ (Hz)	10.94	12.87	—
$J_{\text{exp}}$ (Hz)	9 <sup>b</sup>	9 <sup>b</sup>	9 <sup>b</sup>
$J_{e,\text{lit}}$ (Hz)	6.8 <sup>c</sup>	—	—

<sup>a</sup> For an explanation of the notation, see Table 1, footnote a. The MPW1PW91 functional was used for all calculations presented here. <sup>b</sup> Reference 41,  $J_{\text{HD}}$  measured at 233 K. <sup>c</sup> Reference 18.

**Table 6.** Temperature Dependence of the Results for Complex **3** Using the 6-31G(p) Basis Set for Both Optimization and for Calculation of  $J_{\text{HD}}$ <sup>a</sup>

	0 K	20 K	100 K	200 K	300 K	400 K	600 K
$\Delta r_{\text{HD}}$ (Å)	-0.107	-0.107	-0.118	-0.141	-0.171	-0.205	-0.281
$\langle r_{\text{HD}} \rangle_0$ (Å)	1.174	1.174	1.163	1.140	1.110	1.076	1.000
$\Delta J_e$ (Hz)	3.535	3.538	3.807	4.374	5.141	6.044	8.070
$\Delta J_p$ (Hz)	0.722	0.717	0.416	-0.073	-0.529	-0.942	-1.691
$\Delta J$ (Hz)	4.257	4.255	4.223	4.300	4.612	5.102	6.379
$\langle J \rangle_0$ (Hz)	10.94	10.94	10.91	10.99	11.30	11.79	13.07
$\langle J \rangle^*$ (Hz)	10.95	10.95	10.93	11.04	11.37	11.89	13.21

<sup>a</sup> For further details of the notation, see Table 3, footnote a. The MPW1PW91 functional was used for all calculations presented here.  $J_e$  is 6.69 Hz. The data marked with an asterisk have contributions from hindered methyl rotations removed (35 cm<sup>-1</sup>).

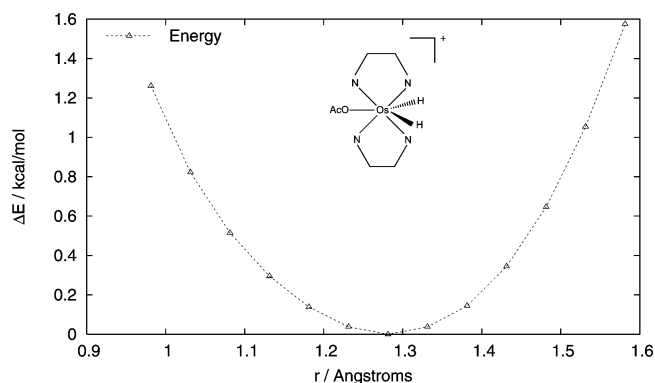
**Table 7.** Temperature Dependence of the Results for Complex **3** Using the IGLO-III Basis Set for Both Optimization and for Calculation of  $J_{\text{HD}}$ <sup>a</sup>

	0 K	20 K	100 K	200 K	300 K	400 K	600 K
$\Delta r_{\text{HD}}$ (Å)	-0.107	-0.107	-0.113	-0.130	-0.153	-0.181	-0.245
$\langle r_{\text{HD}} \rangle_0$ (Å)	1.156	1.156	1.150	1.133	1.110	1.082	1.018
$\Delta J_e$ (Hz)	3.916	3.917	4.088	4.528	5.197	6.020	7.909
$\Delta J_p$ (Hz)	0.661	0.657	0.409	-0.008	-0.389	-0.728	-1.335
$\Delta J$ (Hz)	4.577	4.574	4.496	4.520	4.809	5.292	6.574
$\langle J \rangle_0$ (Hz)	12.87	12.86	12.78	12.81	13.10	13.58	14.86
$\langle J \rangle^*$ (Hz)	12.87	12.87	12.81	12.85	13.16	13.66	14.98

<sup>a</sup> For further details of the notation, see Table 3, footnote a. The MPW1PW91 functional was used for all calculations presented here.  $J_e$  is 8.29 Hz. The data marked with an asterisk have contributions from hindered methyl rotations removed (33 cm<sup>-1</sup>).

why the calculated coupling constants are somewhat too high. For complex **3**, the results are in better agreement with experiment for the calculation of  $\langle J \rangle_0$  with the 6-31G(p) basis set at the 6-31G(p) optimized geometry. Note that this is in contrast to the equilibrium spin–spin coupling constant, where the IGLO-III basis set result is closer to the experimental  $J_{\text{HD}}$ . Because of the large vibrational corrections in this complex an assessment of the computational results based on the equilibrium couplings would lead to the wrong conclusions. The quality of the equilibrium structures, however, heavily influences the vibrationally averaged final result because of the strong dependence of the equilibrium  $J_{\text{HD}}$  on the H–D distance.

Tables 6 and 7 show the temperature dependence of  $r_{\text{HD}}$  and  $J_{\text{HD}}$  for complex **3** using the 6-31G(p) and IGLO-III basis sets, respectively. There is a decrease in the vibrationally averaged H–D distance as temperature increases. Again, this can be attributed to a steeper potential energy surface in the direction of increasing  $r_{\text{HH}}$ . We have verified this observation by plotting

**Figure 5.** Energy of complex **3** as a function of H–H internuclear distance using the 6-31G(p) basis set for the H atoms bound to Os. Each point of the relaxed PES scan has been optimized with the MPW1PW91 hybrid functional.**Table 8.** H–H Equilibrium Distances  $r_e$ , Equilibrium HD Spin–Spin Coupling Constants  $J_e$ , Zero-Point Vibrationally Averaged Values  $\langle r_{\text{HD}} \rangle_0$ ,  $\langle J \rangle_0$ , and Experimental (exp) and Literature (lit) Values for Complex **4**<sup>a</sup>

	4 G//G	4 I//I	4 I//G
$r_e$ (Å)	1.763	1.752	—
$\langle r_{\text{HD}} \rangle_0$ (Å)	1.766	1.755	—
$r_{\text{exp}}$ (Å)	1.76(9) <sup>b</sup>	1.76(9) <sup>b</sup>	1.76(9) <sup>b</sup>
$r_{e,\text{lit}}$ (Å)	1.76 <sup>c</sup>	—	—
$J_e$ (Hz)	-1.09	-0.66	—
$\langle J \rangle_0$ (Hz)	-1.01	-0.53	—
$J_{\text{exp}}$ (Hz)	-0.9 <sup>d</sup>	-0.9 <sup>d</sup>	-0.9 <sup>d</sup>
$J_{e,\text{lit}}$ (Hz)	-1.1 <sup>c</sup>	—	—

<sup>a</sup> For an explanation of the notation, see Table 1, footnote a. The MPW1PW91 functional was used for all calculations presented here. <sup>b</sup> Reference 42. Derived from measured bond angles and atomic distances. <sup>c</sup> Reference 18. <sup>d</sup> Reference 43.

the potential energy as a function of H–H distance, as shown in Figure 5. Consequently, a corresponding increase in the vibrationally averaged  $J_{\text{HD}}$  values is observed as temperature increases from 0 to 600 K. However, as temperature increases, the property curvature correction ( $\Delta J_p$ ) counterbalances a large part of the anharmonicity term. Since the vibrationally averaged H–D distance is influenced solely by the anharmonicity of the potential while the vibrationally averaged HD spin–spin coupling constant is influenced by both the anharmonicity of the potential and the curvature of the  $J$ -coupling surface, it is reasonable to expect that the effect of the property curvature might sometimes cancel out or overpower the effect of the anharmonicity of the potential. To some extent, this is the case for complex **3**. As a consequence, a single calculation of  $J_{\text{HD}}$  at the effective geometry would not yield the correct result.

As with the zero-point vibrationally averaged spin–spin coupling constant, the temperature-dependent vibrational average of  $J_{\text{HD}}$  is in better agreement with experiment when the 6-31G(p) basis set is used for the geometry and property calculation.

**3.4. Complex 4.** Complex **4** is a niobium trihydride complex that has an average experimental value of 1.76(9) Å for  $r_{\text{HH}}$ .<sup>42</sup> Shown in Table 8 is a comparison of our calculated results with experimental and literature data. The zero-point vibrationally averaged  $J_{\text{HD}}$  obtained with the 6-31G(p) basis set is in better agreement with the experimental spin–spin coupling constant

(42) Wilson, R. D.; Koetzle, T. F.; Hart, D. W.; Kvick, A.; Tipton, D. L.; Bau, R. *J. Am. Chem. Soc.* **1977**, *99*, 1775–1781.

(43) Heinekey, D. M. *J. Am. Chem. Soc.* **1991**, *113*, 6074–6077.



**Table 9.** Temperature Dependence of the Results for Complex **4** Using the 6-31G(p) Basis Set for Optimization and for Calculation of  $J_{\text{HD}}^a$ 

	0 K	20 K	100 K	200 K	300 K	400 K	600 K
$\Delta r_{\text{HD}}$ (Å)	0.003	0.003	0.002	-0.001	-0.006	-0.010	-0.020
$\langle r_{\text{HD}} \rangle$ (Å)	1.766	1.766	1.765	1.762	1.757	1.753	1.743
$\Delta J_a$ (Hz)	-0.037	-0.037	-0.041	-0.044	-0.045	-0.045	-0.045
$\Delta J_b$ (Hz)	0.121	0.121	0.115	0.100	0.089	0.087	0.098
$\Delta J$ (Hz)	0.084	0.084	0.074	0.056	0.044	0.042	0.053
$\langle J \rangle$ (Hz)	-1.01	-1.01	-1.02	-1.04	-1.05	-1.05	-1.04
$\langle J \rangle^*$ (Hz)	-1.01	-1.01	-1.02	-1.03	-1.04	-1.04	-1.02

<sup>a</sup> For further details of the notation, see Table 3, footnote a. The MPW1PW91 functional was used for all calculations presented here.  $J_c$  is -1.09 Hz. The data marked with an asterisk have a contribution from normal mode 1 (56 cm<sup>-1</sup>) removed (Cp rotations).

**Table 10.** Temperature Dependence of the Results for Complex **4** Using the IGLO-III Basis Set for Optimization and for Calculation of  $J_{\text{HD}}^a$ 

	0 K	20 K	100 K	200 K	300 K	400 K	600 K
$\Delta r_{\text{HD}}$ (Å)	0.003	0.003	0.002	-0.001	-0.005	-0.010	-0.019
$\langle r_{\text{HD}} \rangle$ (Å)	1.755	1.755	1.754	1.751	1.747	1.742	1.733
$\Delta J_a$ (Hz)	-0.043	-0.044	-0.047	-0.048	-0.047	-0.044	-0.037
$\Delta J_b$ (Hz)	0.169	0.169	0.162	0.148	0.140	0.143	0.168
$\Delta J$ (Hz)	0.125	0.125	0.116	0.100	0.093	0.099	0.131
$\langle J \rangle$ (Hz)	-0.53	-0.53	-0.54	-0.56	-0.56	-0.56	-0.52
$\langle J \rangle^*$ (Hz)	-0.53	-0.53	-0.54	-0.55	-0.55	-0.54	-0.50

<sup>a</sup> For further details of the notation, see Table 3, footnote a. The MPW1PW91 functional was used for all calculations presented here.  $J_c$  is -0.66 Hz. The data marked with an asterisk have a contribution from normal mode 1 (56 cm<sup>-1</sup>) removed (Cp rotations).

of -0.9 Hz, which is consistent with the results obtained for the zero-point vibrational average of the H-D internuclear distance. The 6-31G(p) basis yields better agreement with experiment for the H-H distance and the  $J_{\text{HD}}$  spin-spin coupling constant. For both basis sets, the zero-point vibrationally averaged  $r_{\text{HD}}$  is very close to the respective equilibrium distance. Likewise, the zero-point vibrational correction to  $J_{\text{HD}}$  is also relatively small in this complex.

Tables 9 and 10 show the temperature dependence of  $J_{\text{HD}}$  for complex **4**. The temperature dependence of the vibrational averages of  $r_{\text{HD}}$  and  $J_{\text{HD}}$  indicates that there is little or no change as temperature increases. As a result,  $\langle J \rangle$  remains about the same as temperature increases. This result is due to the fact that the potential is relatively harmonic (as illustrated by the small changes in  $\langle r_{\text{HD}} \rangle$  as temperature increases) and that the  $J$ -coupling surface has a small curvature. Therefore, a very small  $J$  does not necessarily indicate that vibrational contributions will be large in comparison. The zero-point vibrational correction for free HD is about 5% of the equilibrium value of 43 Hz.<sup>19</sup> Absolute vibrational corrections of the same magnitude would obviously be completely dominating the coupling constants for all complexes with large  $r_{\text{HH}}$ . Instead, we see that for complex **4** there is no longer a shallow anharmonic potential present along the H-D coordinate that would cause vibrational corrections on the order of several Hz as was the case for the other complexes where the H-D bond is still intact to some degree. The sign change of the coupling constant further indicates that the H-D coupling should be viewed as a two-bond coupling mediated by the metal.

**3.5. Complex 5.** Complex **5** is a dihydride rhenium complex for which an experimental  $r_{\text{HH}}$  of 1.27 Å was estimated in ref 44 from the longitudinal relaxation times in the proton NMR. In the same paper, a coupling constant  $J_{\text{HD}}$  of 12.8 Hz measured

**Table 11.** H-H equilibrium Distances  $r_e$ , Equilibrium HD Spin-Spin Coupling Constants  $J_e$ , Zero-Point Vibrationally Averaged Values  $\langle r_{\text{HD}} \rangle_0$ ,  $\langle J \rangle_0$ , and Experimental (exp) and Literature (lit) Values for Complex **5**<sup>a</sup>

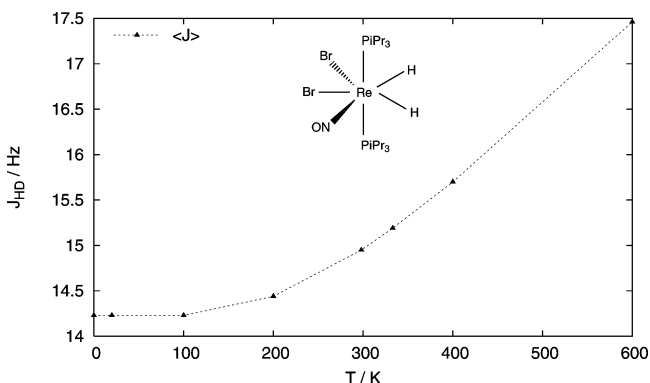
	5
	G/G
$r_e$ (Å)	1.343
$\langle r_{\text{HD}} \rangle_0$ (Å)	1.236
$r_{\text{exp}}$ (Å)	1.27 <sup>b</sup>
$r_{\text{e.lit}}$ (Å)	1.33 <sup>c</sup>
$J_e$ (Hz)	9.52
$\langle J \rangle_0$ (Hz)	14.23
$J_{\text{exp}}$ (Hz)	12.8 <sup>b</sup>
$J_{\text{e.lit}}$ (Hz)	9.8 <sup>c</sup>

<sup>a</sup> For an explanation of the notation, see Table 1, footnote a. The MPW1PW91 functional was used for all calculations presented here. <sup>b</sup> Reference 44,  $J_{\text{HD}}$  measured at room temperature. <sup>c</sup> Reference 18.

**Table 12.** Temperature Dependence of the Results for Complex **5** Using the 6-31G(p) Basis Set for Both Optimization and for Calculation of  $J_{\text{HD}}^a$ 

	0 K	20 K	100 K	200 K	300 K	400 K	600 K
$\Delta r_{\text{HD}}$ (Å)	-0.108	-0.108	-0.127	-0.133	-0.148	-0.170	-0.221
$\langle r_{\text{HD}} \rangle$ (Å)	1.236	1.236	1.217	1.211	1.196	1.174	1.123
$\Delta J_a$ (Hz)	3.503	3.501	3.461	3.539	3.839	4.281	5.380
$\Delta J_b$ (Hz)	1.207	1.208	1.246	1.376	1.606	1.896	2.561
$\Delta J$ (Hz)	4.710	4.709	4.707	4.915	5.445	6.178	7.941
$\langle J \rangle$ (Hz)	14.23	14.23	14.23	14.44	14.97	15.70	17.46

<sup>a</sup> For further details of the notation, see Table 3, footnote a. The MPW1PW91 functional was used for all calculations presented here.  $J_c$  is 9.52 Hz. <sup>b</sup> Experimental data in C<sub>6</sub>D<sub>6</sub>: 12.75 Hz (25 °C), 12.83 (30), 12.90 (40), 12.97 (50), 13.07 (60), ref 45. Calculated: 14.95 Hz (25 °C), 15.19 (60).

**Figure 6.** H-D spin-spin coupling of complex **5** as a function of temperature (MPW1PW91 hybrid functional). The 6-31G(p) basis set has been for the H atoms bound to Re.

at room temperature was reported. The authors also employed the empirical  $J_{\text{HD}}$ -versus- $r_{\text{HH}}$  relation from ref 13 to arrive at an estimated  $r_{\text{HH}}$  of 1.21 Å. Recently, Gusev<sup>45</sup> has measured the temperature dependence of  $J_{\text{HD}}$  for this system in C<sub>6</sub>D<sub>6</sub> as 12.75 Hz (25 °C), 12.83 (30), 12.90 (40), 12.97 (50), 13.07 (60), with an estimated uncertainty of less than 0.1 Hz. Measurements for a larger temperature range are under way. Our results obtained with the 6-31G(p) basis for the H ligands are collected in Tables 11 and 12. The calculated  $\langle J_{\text{HD}} \rangle_0$  and  $\langle r_{\text{HD}} \rangle_0$  are in reasonable agreement with experimental data. The calculated temperature trend shown in Figure 6 is compatible with the experiment. Between 25 and 60 °C,  $J_{\text{HD}}$  increases by about 0.24 Hz, which is within the estimated experimental

(44) Gusev, D.; Llamazares, A.; Artus, G.; Jacobsen, H.; Berke, H. *Organometallics* **1999**, *18*, 75–89.

(45) Gusev, D. G. Private communication.

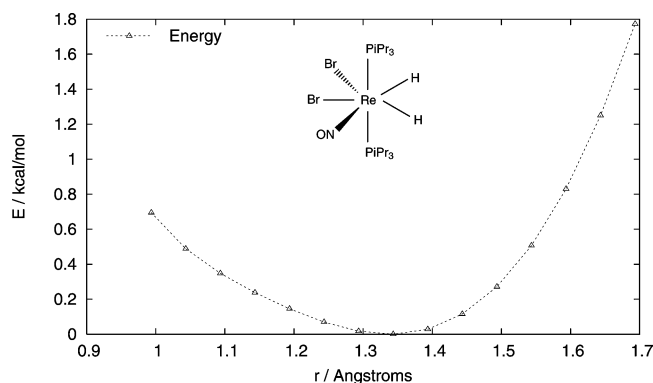


**Figure 7.** Energy of complex **5** as a function of H–H internuclear distance using the 6-31G(p) basis set for the H atoms attached to Re. Each point of the relaxed PES scan has been optimized with the MPW1PW91 functional.

uncertainties. For the zero-point vibrationally averaged H–D distance a sizable negative shift away from the equilibrium distance is found, along with a large vibrational correction of almost 5 Hz on  $J_{\text{HD}}$ . Considering the experimental estimates for  $r_{\text{HH}}$ , it appears that our calculated averaged  $\langle r_{\text{HD}} \rangle$  is slightly too low which we tentatively attribute to an underestimation of the equilibrium distance. As a consequence, an underestimation of  $\langle r_{\text{HD}} \rangle$  rationalizes the overestimation of  $\langle J_{\text{HD}} \rangle$  compared to experiment. As in the case of complex **3** the quality of the equilibrium structure turns out to be a critical factor.

The potential energy surface for complex **5** is shown in Figure 7. It is seen to be strongly anharmonic, which explains the large zero-point vibrational corrections for the H–D distance. Additional finite temperature corrections to  $\langle r_{\text{HD}} \rangle$  are pronounced, with a 0.04 Å decrease from 0 to 300 K. The large vibrational effects on  $J_{\text{HD}}$  are to a large extent attributable to the difference between  $r_e$  and  $\langle r_{\text{HD}} \rangle$  at 0 K (see Table 12; the property curvature term contributes only about one-third of the total vibrational corrections). The calculated increase of  $J_{\text{HD}}$  with  $T$  is moderately strong and is seen to be caused by both the property curvature and the anharmonicity terms. At 300 K, the temperature effects on  $\langle J_{\text{HD}} \rangle$  almost amount to an additional 1 Hz. It is possible that, due to the strong anharmonicity of the PES as shown in Figure 7, vibrational corrections from higher than cubic terms in the potential and higher-order property derivatives might not be negligible here. However, the major portion of the vibrational correction is likely to be covered by the terms considered in our calculations. Overall, the calculated average H–D distance is in good agreement with the experimental estimate of 1.21 Å from ref 44 based on the  $J_{\text{HD}}$  measurement, and the calculated temperature dependence above 300 K is in agreement with the recent observations by Gusev.<sup>45</sup>

**3.6. Complex 6.** To our knowledge, experimental data for  $J_{\text{HD}}$  of the Ru complex **6** are not available. In ref 8, complex **6** has been used as a theoretical model for the complex  $[\text{Ru}(\text{Cp}^*)\text{-(dppm)}\text{H}_2]^+$  (**7**, dppm = bis(diphenylphosphino)methane). Due to the large dppm ligand and the five methyl groups of the  $\text{Cp}^*$  ligand, complex **7** is a particularly expensive system computationally. For **7**, the experimental  $r_{\text{HH}}$  is 1.10 Å as determined from neutron diffraction.<sup>46</sup> A pronounced temperature dependence of the H–D spin–spin coupling was also reported in ref 46. This, and a range of related  $\text{Ru}(\text{R}_2\text{P-R}'\text{-PR}_2)(\text{Cp}/\text{Cp}^*)^+$

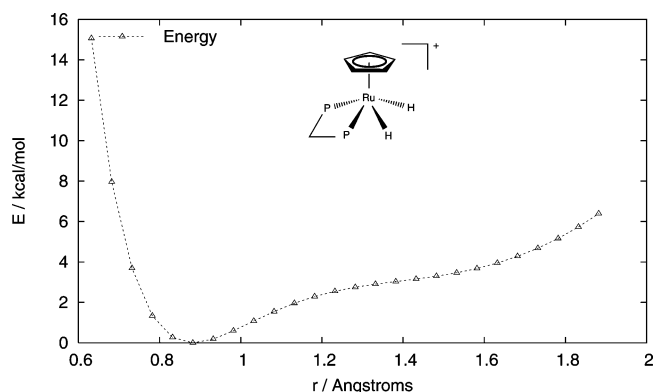


**Figure 8.** Energy of complex **6** as a function of H–H internuclear distance using the 6-31G(p) basis set for the H atoms attached to Ru. Each point of the relaxed PES scan has been optimized with the B3LYP functional.

complexes were recently investigated by Law, Mellows, and Heinekey in ref 47. Law et al. determined  $r_{\text{HD}}$  from the empirical relation between  $r_{\text{HD}}$  and  $J_{\text{HD}}$  of ref 12 to be within 1.060(5) and 1.091(5) Å for temperatures ranging from 204 to 286 K. At room temperature, the empirical relation devised by Maltby et al.<sup>13</sup> yielded a slightly shorter  $r_{\text{HD}}$  of 1.071 Å.

The authors of ref 8 studied the temperature dependence of  $J_{\text{HD}}$  for **7** (22.3 to 21.1 Hz from 213 to 295 K as determined in ref 46) theoretically by using calculations of the temperature dependence of the H–D distance in complex **6** to model this behavior. The empirical relation of Maltby et al.<sup>13</sup> between  $J_{\text{HD}}$  and  $r_{\text{HD}}$  was employed in the “reverse” way, i.e.,  $\langle r_{\text{HD}} \rangle$  averaged with a nuclear vibrational wave function obtained for a two-dimensional subspace was used to calculate the resulting  $J_{\text{HD}}$ . The temperature-dependent vibrational average of  $J_{\text{HD}}$  was not directly calculated in ref 8 with this wave function (as it was possible 7 years later for complex **1**). Based on the temperature-dependent change in  $\langle r_{\text{HD}} \rangle$ , remarkably good agreement with the experimentally observed decrease of  $J_{\text{HD}}$  was obtained.

It should be noted that the experimental work by Law et al. in 2002<sup>47</sup> considered several  $\text{Ru}(\text{R}_2\text{P-R}'\text{-PR}_2)(\text{Cp}/\text{Cp}^*)^+$  complexes differing in the bis-phosphino ligand among which **7** ( $\text{R}' = \text{CH}_2$ ) had the strongest temperature dependence. Two other complexes exhibited a noticeable but less pronounced decrease of  $J_{\text{HD}}$  with  $T$  ( $\text{R}' = \text{C}_2\text{H}_4$ ), whereas another complex with  $\text{R}' = \text{C}_3\text{H}_6$  exhibited a slight increase in  $J_{\text{HD}}$  with temperature. This shows that the exact nature of the bis-phosphino ligand plays an important role for the temperature dependence of this class of complexes.

The PES for the model complex **6** has a complicated shape, as was already found by the authors of ref 6. The energy of **6** as a function of H–H distance is shown in Figure 8 (6-31G(p) basis for the H ligands, all other coordinates optimized). The IGLO-III result is similar and can be found in the Supporting Information. It should be noted that the path on the PES shown in Figure 8 does not simply follow the H–D stretching mode but involves significant changes of the metal–HD distance as well as other coordinates. At large  $r_{\text{HH}}$  (around 1.4 Å) there is almost a plateau which is only about 3 kcal/mol above the PES minimum. From fitting the data in Figure 8 we have estimated that an expansion of the PES around the minimum including terms up to sixth power would be necessary to capture this

(46) Klooster, W. T.; Koetzle, T. F.; Jia, G.; Fong, T. P.; Morris, R. H.; Albinati, A. *J. Am. Chem. Soc.* **1994**, *116*, 7677–7681.

(47) Law, J. K.; Mellows, H.; Heinekey, D. M. *J. Am. Chem. Soc.* **2002**, *124*, 1024–1030.

**Table 13.** H–H Equilibrium Distances  $r_e$ , Equilibrium HD Spin–Spin Coupling Constants  $J_e$ , Zero-Point Vibrationally Averaged Values  $\langle r_{\text{HD}} \rangle_0$ ,  $\langle J \rangle_0$ , and Experimental (exp) and Literature (lit) Values for Complex **6**<sup>a</sup>

	6 G//G	6 l//l
$r_e$ (Å)	0.882	0.892
$\langle r_{\text{HD}} \rangle_0$ (Å)	0.891	0.905
$r_{\text{exp}}$ (Å) <sup>b</sup>	1.10	1.10
$r_{e,\text{lit}}$ (Å) <sup>c</sup>	0.888	—
$J_e$ (Hz)	34.43	32.94
$\langle J \rangle_0$ (Hz)	34.38	32.59
$J_{\text{exp}}$ (Hz) <sup>d</sup>	20.6(3)	20.6(3)
$J_{e,\text{lit}}$ (Hz)	—	—

<sup>a</sup> For an explanation of the notation, see Table 1, footnote a. The B3LYP functional was used for all calculations presented here. <sup>b</sup> For complex **7**, ref 46. A  $J_{\text{HD}}$ -derived distance for **7** from ref 47 is 1.091 Å. <sup>c</sup> Reference 8. <sup>d</sup> For complex **7**, ref 47.

**Table 14.** Temperature Dependence of the Results for Complex **6** Using the 6-31G(p) Basis Set for Both Optimization and for Calculation of  $J_{\text{HD}}$ <sup>a</sup>

	0 K	20 K	100 K	200 K	300 K	400 K	600 K
$\Delta r_{\text{HD}}$ (Å)	0.009	0.009	0.008	0.003	−0.005	−0.015	−0.038
$\langle r_{\text{HD}} \rangle$ (Å)	0.891	0.891	0.890	0.885	0.877	0.867	0.844
$\Delta J_a$ (Hz)	0.021	0.020	0.018	0.076	0.212	0.398	0.850
$\Delta J_b$ (Hz)	−0.076	−0.075	−0.049	−0.018	−0.006	−0.012	−0.057
$\Delta J$ (Hz)	−0.055	−0.055	−0.031	0.058	0.206	0.386	0.793
$\langle J \rangle$ (Hz)	34.38	34.38	34.40	34.49	34.64	34.82	35.23
$\langle J \rangle^*$ (Hz)	34.37	34.37	34.37	34.37	34.55	34.70	35.05

<sup>a</sup> For further details of the notation, see Table 3, footnote a. The B3LYP hybrid functional was used for all calculations presented here.  $J_e$  is 34.43 Hz. The data marked with an asterisk have the contribution from normal mode 1 (45 cm<sup>−1</sup>) removed (Cp rotations).

behavior correctly. The “plateau” region is critical for obtaining the large difference between  $\langle r_{\text{HD}} \rangle$  (experiment: around 1.10 Å at room temperature) and the equilibrium H–D distance of 0.88 Å. As seen in our calculated data in Table 14 the cubic anharmonic terms resulting from a normal mode expansion around the minimum are in fact very small compared to those of the other complexes studied here and lead only to a small vibrational correction for the geometry. The “near-sighted” cubic expansion around the PES minimum is evidently not capable of describing the large vibrational corrections that are obtained from solving the nuclear Schrödinger equation explicitly. If an actual minimum were present around an H–D separation of 1.4 Å, we would be able to treat this complex in the same way as complex **1**. A second local minimum would likely cause the decrease of  $J_{\text{HD}}$  with temperature to be even stronger than what was found experimentally for complex **7** (similar to **1**). We can roughly estimate the strong zero-point correction to  $r_{\text{HD}}$  in our method by applying a large displacement on the order of 0.1 Å for calculating the numerical derivatives along the two normal modes that yield most of the vibrational corrections (Ru–HD and H–D stretching modes, see Figure 9). In this way, a large anharmonicity of the PES is detected by the calculation in an approximate, average sense and leads to  $\langle r_{\text{HD}} \rangle_0$  of larger than 1 Å. However, this calculation predicts that  $\langle r_{\text{HD}} \rangle$  decreases slightly with increasing temperature. We attribute this behavior to the population of higher states in lower-energy normal modes that have a potential similar to the one shown for normal mode 22 in Figure 9. Since the energy of this lower-frequency normal mode is steeper in the direction of increasing  $r_{\text{HD}}$ , the slight decrease in the vibrationally averaged  $\langle r_{\text{HD}} \rangle$  as temperature increases is observed. Therefore, it appears that the anharmonic

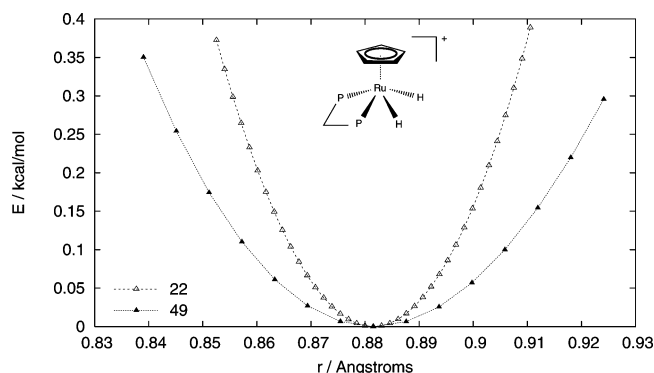


**Figure 9.** Energies of complex **6** displaced along the normal modes no. 22 (811 cm<sup>−1</sup>; mainly Ru–HD stretch) and 49 (2311 cm<sup>−1</sup>; mainly H–D stretch) as a function of the H–H internuclear distance using the 6-31G(p) basis set for the H atoms attached to Ru. The B3LYP hybrid functional has been used in these calculations presented here.

nicity terms higher than third order need to be considered properly in the calculations to yield the correct temperature dependence of  $\langle r_{\text{HD}} \rangle$  and  $\langle J_{\text{HD}} \rangle$ .

An issue that might further complicate accurate ab initio computations of  $J_{\text{HD}}$  for complex **6** is a pronounced sensitivity of the property surface near the minimum with respect to the basis set. Calculated  $J_{\text{HD}}$  as a function of H–D distance along the same relaxed path on the PES as the potential shown in Figure 8 can be found in the Supporting Information. Both the slope and the curvature of  $J_{\text{HD}}$  vs  $r_{\text{HD}}$  have opposite signs for the two basis sets near the minimum at  $r_{\text{HD}} = 0.88/0.89$  Å, respectively. Consequently, we found similar sign changes for the property derivatives with respect to the H–D stretching normal mode. This behavior indicates that, despite the vibrational effects on  $r_{\text{HD}}$  being similar with both basis sets, it will be difficult to obtain averaged values for  $J_{\text{HD}}$  that are consistent between basis sets. Changes in the property surface will not affect just our method but would also influence the results from a full or reduced-dimension quantum nuclear dynamics method, although it is obvious that an expansion around the PES minimum will be more sensitive to local errors. The sensitivity of the property surface for model complex **6** may provide a hint for explaining why the different Ru(R<sub>2</sub>P–R′–PR<sub>2</sub>)(Cp/Cp\*)<sup>+</sup> complexes exhibit a somewhat different temperature dependence of  $J_{\text{HD}}$ .

#### 4. Summary and Conclusions

Vibrational corrections on  $J_{\text{HD}}$  in metal hydride and dihydrogen complexes are of high significance. For free H–D, the correction is on the order of 2–3 Hz or 5% of the experimental value.<sup>19</sup> Computations that attempt to reproduce the experiment within a reasonable margin of error as, for instance, expected from hybrid DFT calculations may neglect corrections of a few percent for qualitative (semiquantitative) analyses and interpretations of trends and magnitudes of  $J_{\text{HD}}$ . One should expect that for elongated dihydrogen and compressed hydride complexes the relative importance of vibrational corrections to  $J_{\text{HD}}$  might far exceed the 5% calculated for free dihydrogen. The first reason is the strong dependence of  $J_{\text{HD}}$  on the H–D distance. A neglected 2–3 Hz correction of a small H–D coupling constant found in an elongated dihydrogen complex can render a computational analysis of  $J_{\text{HD}}$  highly questionable or even useless. Second, in the highly interesting regime where the H–D

bond is still (partially) intact but severely elongated the increased PES anharmonicity can potentially cause larger (absolute) vibrational corrections as found in free dihydrogen. This work as well as the computational studies by Lluch, Lledos, et al. cited previously shows that this is the case. Attempts to verify and improve the important relationships between  $J_{\text{HD}}$  and  $r_{\text{HH}}$  with the help of first-principles theory must therefore take vibrational corrections into consideration. Of course, for medium- to high-accuracy computations a 5% correction must also not be neglected.

It has been unclear yet if the small  $J_{\text{HD}}$  in hydride complexes with large H–H separations are severely affected by vibrational corrections. Computations have shown that a number of coupling constants on the order of 0–1 Hz observed for such systems are negative.<sup>19,18</sup> Vibrational corrections of 2–3 Hz would be able to change the sign, or increase the magnitude of  $J_{\text{HD}}$  by a factor of 2–3, depending on the sign of the vibrational corrections. Our results for complex **4** indicate that for hydride complexes with large H–D separations and small negative  $J_{\text{HD}}$  on the order of 1 Hz the vibrational corrections probably do not exceed 0.1 Hz because of a rather harmonic PES. The negative coupling constant should be considered a three-bond coupling mediated by the metal. Despite the fact that the metal's valence shell mediates the H–D coupling, spin–orbit effects on  $J_{\text{HD}}$  were previously shown to be small for such complexes.<sup>19</sup>

Regarding an actual or possible temperature dependence of  $J_{\text{HD}}$ , from the results presented in the previous section we may assign the complexes studied in the previous section to various classes:

1. Complexes with a very strong temperature dependence of  $J_{\text{HD}}$  due to an equilibrium between two isomers that have strongly different  $J_{\text{HD}}$ . Example: complex **1**.

2. Complexes with a small-to-moderate temperature dependence of  $J_{\text{HD}}$  due to temperature-dependent vibrational corrections of  $J_{\text{HD}}$  for a single structure. The reason is a strongly anharmonic PES with a partially intact H–D bond and/or large property curvature effects. Examples: complexes **2**, **3**, **5**, **6**. For complex **2**, the temperature dependence of the H–T coupling might be too small to be reliably detectable between 125 and 200 K.

3. In some cases a small-to-moderate temperature dependence of  $J_{\text{HD}}$  may result despite a highly anharmonic PES due to a partial or almost complete temperature dependence of anharmonicity and property curvature terms in the vibrational average of  $J_{\text{HD}}$ . For complex **3** we find a partial cancellation of pronounced temperature effects. It is conceivable that in other complexes the cancellation is nearly complete.

4. Complexes with a very small temperature dependence of  $J_{\text{HD}}$  due to (a) a relatively harmonic PES and resulting small property curvature terms in the vibrational average of  $J_{\text{HD}}$  (in this case the zero-point corrections might also be small) or (b) little temperature dependence of sizable anharmonicity and property curvature terms. Example: complex **4**.

We may further subdivide class 2 into cases where either the property curvature or the anharmonicity effects are dominant. Complex **6** represents a transition between classes 1 and 2. If the potential energy in the dihydride region were a little lower, the second minimum would likely cause a strong temperature dependence of  $J_{\text{HD}}$  that we could treat in the same way as for complex **1**. The complicated shape of the PES and sensitivity

of the  $J_{\text{HD}}$  surface make this system very challenging for computations. We expect that other members of the diverse sets of complexes computed recently by Gusev<sup>18</sup> and by us<sup>19</sup> fall into one of these classes. By including vibrational corrections for each of these complexes we will be able to obtain a much better assessment of the performance of hybrid and nonhybrid DFT in predictions of  $J_{\text{HD}}$  for metal dihydrogen and dihydride complexes.

With the advancement of efficient algorithms for computing NMR spin–spin coupling constants and the prevalence of computational clusters, it is becoming easier to calculate accurate vibrationally averaged  $J_{\text{HD}}$  from first principles. It is evident from the data presented here that the zero-point vibrational correction contributes greatly to the overall vibrational average for all complexes and needs to be included in computations. Thermal population of additional vibrationally excited states can result in a noticeable temperature dependence of both  $\langle r_{\text{HD}} \rangle$  and  $\langle J_{\text{HD}} \rangle$ . According to our calculations, complexes **3** and **5**, and to some extent complex **2**, should exhibit a more or less pronounced temperature dependence of  $\langle r_{\text{HD}} \rangle$  and  $J_{\text{HD}}$ , unless yet neglected higher-order perturbational corrections in the theoretical treatment unexpectedly are able to completely cancel these trends. For **5**, preliminary experimental data<sup>45</sup> confirm an increase of  $J_{\text{HD}}$  with temperature as predicted here.

Although it has been discovered previously that the H–D spin–spin coupling constant of complex **1** has an unusual temperature dependence due to the existence of two minima that have a relatively small energy gap and a low isomerization barrier, we have shown that these minima can be treated as separate species computationally. The Boltzmann average of the zero-point averaged values of  $J_{\text{HD}}$  for the two structures can then be used to construct the temperature dependence of the spin–spin coupling constant for this complex which is in good agreement with experiment. We have shown that low-frequency vibrations influence this temperature dependence in several ways, most notably by their contribution to the zero-point energy difference between the two isomers.

A potential energy surface demonstrating a steeper increase of the energy in the direction of increasing H–H distance is a known characteristic for compressed dihydrides.<sup>18,16</sup> We have shown that complex **2** (a trihydride complex) and complex **3** (an elongated dihydrogen complex) also exhibit this behavior. Further, complex **3** has illustrated that anharmonicity and property curvature corrections are equally important in considering vibrationally averaged values for the HD spin–spin coupling constant. Although the vibrational average for  $r_{\text{HD}}$  decreases with increasing temperature, the vibrational average for  $J_{\text{HD}}$  does not increase correspondingly due to the larger influences of the property curvature term. This shows that vibrationally averaged structures are not sufficient enough to predict the vibrational average of  $J_{\text{HD}}$ . It is important to consider both the anharmonicity and the property curvature simultaneously.

Deciding which basis set yields better agreement with experiment with respect to both geometry and spin–spin coupling calculations appears to be somewhat difficult. For free dihydrogen, the IGLO-III basis is clearly superior (e.g. for  $\langle J_{\text{HD}} \rangle_0$ , B3LYP/6-31G(p): 53.53 Hz; B3LYP/IGLO-III: 45.48 Hz; expt: 42 Hz), but for the metal complexes the situation is different. In the case of complex **1**, the 6-31G(p) basis set predicts an energy difference which yields good agreement with

experiment for  $J_{\text{HD}}$ . Using the IGLO-III basis set for this complex would not yield a strong enough temperature dependence, owing to the larger energy gap between the two isomers of the complex calculated at the IGLO-III level. It was previously reported in ref 16 that, for **1**, both basis sets yield similar equilibrium couplings, which is confirmed by our study. For the other complexes where we made a comparison, both basis sets yield acceptable agreement with experiment, with a tendency of the 6-31G(p) results being closer to experiment. It would also appear that the 6-31G(p) basis set is slightly superior when comparing  $\langle r_{\text{HD}} \rangle_0$  and experimental geometries.

**Acknowledgment.** We acknowledge support from the Center for Computational Research (CCR) at the University at Buffalo. B.C.M. thanks the United States Department of Defense for support through a National Defense Science and Engineering Graduate (NDSEG) Fellowship. J.A. is grateful for financial

support from the ACS Petroleum Research Fund and from the CAREER program of the National Science Foundation (CHE-0447321). We thank Dr. Serguei Patchkovskii and Prof. D. Michael Heinekey for helpful comments. We are grateful to Prof. Dmitri G. Gusev for suggesting the study of complex **5** and for providing us with unpublished variable-temperature NMR data for this complex. We also thank an anonymous reviewer for constructive comments.

**Supporting Information Available:** Details of the procedure used for the vibrational averaging; additional computational results for complexes **1**, **2**, and **6**; complete citations for refs 23 and 30. This material is available free of charge via the Internet at <http://pubs.acs.org>.

JA0586236